ISSN: 2414-1895 DOI: 10.6919/ICJE.202304_9(4).0051

Research on MoS_2-MXene/S in Cathode Materials for Lithium-Sulfur Batteries

Zhe Gao[a], Zhulong Wang[b] and Guoqing Sun[c]

School of Shipping, Shandong Jiaotong University, Weihai 264200, China

[a]1453838107@qq.com, [b]155300125@qq.com, [c]17863025676@163.com

Abstract

In recent years, with the rapid growth of global new energy chemical power supply market demand, lithium-sulfur-ion batteries are regarded as the most feasible next-generation energy storage system to replace resource-scarce lithium-ion batteries because of their large specific energy, high specific capacity, and inexhaustible resources, safety, and ecological friendliness. However, the serious shuttle effect and the rapid capacity decay and low actual energy density caused by poor conductivity of the sulfur cathode affect its development, so the design of reasonable cathode materials is one of the effective strategies to solve the above problems. In this paper, MXene was compounded with molybdenum disulfide (MoS_2) and the material characterization and electrochemical performance of the prepared cathode material were tested, and the experimental results showed that MoS_2-$Ti_3C_2T_x$ retained the advantages of high specific surface area and pore volume of $Ti_3C_2T_x$ two-dimensional materials, while the doping of molybdenum further improved the conductivity and adsorption performance of polysulfides of cathode materials. The sulfur content in MoS_2-$Ti_3C_2T_x$/S composites is as high as 70.2%, and the initial discharge specific capacity of 1057 mAh·g^{-1} is obtained at 0.2 C rate current, which is still maintained at 758.6 mAh·g^{-1} after 100 cycles, which is 71.7% of the initial discharge capacity. The MoS_2-$Ti_3C_2T_x$ electrode idea proposed in this paper provides a reference for the realization of low-cost and high-energy density lithium-sulfur batteries.

Keywords

Lithium-sulfur Batteries; Shuttle Effect; MoS_2-$Ti_3C_2T_x$; Cathode Composites.

1. Introduction

In recent years, with the rapid growth of global demand for new energy chemical power supply market, human demand for energy is increasing. The energy crisis caused by the depletion of non-renewable fossil fuels (such as coal, oil and gas) and global environmental problems such as air pollution are two major problems for the sustainable development of human society today[1,2]. Therefore, human beings urgently need to develop renewable clean energy (such as solar energy, wind energy, tidal energy, geothermal energy, etc.), but these clean energy usually have the characteristics of volatility and intermittency, and need to be converted by energy storage and conversion devices before they can be widely used in portable electronic devices, smart grids and unmanned ships[3]. At present, the high-efficiency and pollution-free electrochemical energy storage system has been widely concerned by scientific researchers, and in order to better use these clean energy, people have put forward the requirements of safety, low cost, high energy density and long cycle life of the electrochemical energy storage system[4].

ISSN: 2414-1895 DOI: 10.6919/ICJE.202304_9(4).0051

Among many battery systems, lithium-sulfur batteries using elemental sulfur as the positive active material and lithium metal as the negative electrode have become one of the most promising electrochemical energy storage devices with their ultra-high theoretical energy density (2576 $Wh \cdot kg^{-1}$) and theoretical specific capacity (1675 $mAh \cdot g^{-1}$)[5]. In addition, it has the advantages of extensive resources, low cost, safety and reliability, and green cleaning [6.7]. However, at present, the development of lithium-sulfur batteries still faces many challenges such as poor conductivity of cathode materials and discharge products, "shuttle effect", and sulfur-cathode volume expansion [7]. Among them, the "shuttle effect" is the main factor leading to the performance degradation of lithium-sulfur batteries. In order to suppress the shuttle effect, sulfur and host materials can be used to build a lithium-sulfur battery cathode to anchor the polysulfide, thereby overcoming the above problems. The two-dimensional material has a large specific surface area and strong mechanical stability, which is suitable as an anchoring material for lithium-sulfur batteries. It is still affected by problems such as rapid capacity decay, low actual energy density and poor cycle life. The main causes of these problems are the shuttle effect of polysulfides and the poor conductivity of sulfur. Therefore, designing solutions that effectively suppress the shuttle effect and improve conductivity at the same time is the key to promoting the rapid development of lithium-sulfur batteries [8].

According to numerous studies, the development of suitable cathode composites is one of the effective solutions, and carbon materials are one of the important carrier materials for sulfur cathodes in lithium-sulfur batteries [9]. On the one hand, carbon materials have a huge surface area and abundant pores, which can "fix" Li_2S_n in the pores and play the role of physical sulfur fixation; On the other hand, the good conductivity of carbon materials is conducive to improving the electron transport rate and electrochemical reaction efficiency. Transition metal sulfides are also one of the more studied cathode carrier materials for lithium-sulfur batteries. It is found that there is a strong interaction between MoS_2 and Li_2S_n, which can anchor Li_2S_n to the surface and promote the mutual conversion of Li_2S_n, thereby inhibiting the "shuttle effect" and improving the rate performance and cycle performance of lithium-sulfur batteries [10]. However, because its non-sexual surfaces interact weakly with LiPSs, they need to be further modified. $Ti_3C_2T_x$-MXene (T-F, =O, and -OH groups) is a member of two-dimensional transition metal carbides with excellent electrical conductivity, and its surface energy for chemical adsorption of LiPSs by Lewis acids makes it suitable for modifying carbon carriers[11]. In this paper, $Ti_3C_2T_x$ nanosheets were obtained by etching $Ti_3C_2T_x$ and introduced into molybdenum disulfide (MoS_2), and MoS_2/S composites were constructed, and $Ti_3C_2T_x$ nanosheets dispersed inside MoS_2/S particles could act as conductive bridges and accelerate electron transport inside the electrodes. In addition, the unique two-dimensional structure of $Ti_3C_2T_x$ can also form multiple LiPSs adsorption and barrier regions, which effectively hinders their diffusion.

2. Experimental Methods

2.1 Reagents & Instruments

Sublimation sulfur (analytical pure, Chengdu Kelong Chemical Co., Ltd.), concentrated hydrochloric acid (analytical pure, Yantai Shuangshuang Chemical Co., Ltd.), lithium fluoride (analytical pure, Tianjin Jinhui Taiya Chemical Reagent Co., Ltd.), titanium aluminum carbide (99.5%, Foshan Xinene Technology Co., Ltd.), ammonium molybdate tetrahydrate (AMT) (analytical pure, Aladdin Biotechnology Co., Ltd.), thiourea (analytical pure, Beijing Bailinway Technology Co., Ltd.), sulfur powder (analytical pure, Beijing Bailinway Technology Co., Ltd.), polypropylene film (battery grade, Shenzhen Tianchenghe Technology Co., Ltd.), polyvinylidene fluoride (battery grade, Dongguan Zhanyang Polymer Materials Co., Ltd.), N-methylpyrrolidone (analytical pure, Tianjin Beilian Fine Chemicals Development Co., Ltd.)

Scanning electron microscopy (SEM) was used to observe the microstructure of materials, X-ray diffractometer (XRD) to detect the crystal structure of materials, thermogravimetric analysis (TGA) to determine sulfur content, and water droplet contact angle to determine the wettability of electrode and electrolyte. The specific capacity, rate performance and impedance of the battery are tested by

ISSN: 2414-1895 DOI: 10.6919/ICJE.202304_9(4).0051

constant current charge and discharge test (GCD), cyclic voltammetry test (CV), and alternating current impedance test (EIS).

2.2 $Ti_3C_2T_x$ Preparation

First, 1 g of LiF was added to 20 mL of HCl (9 mol· L^{-1}) and stir until completely dissolved. Subsequently, 1 g of Ti_3AlC_2 powder was slowly added to the mixed solution, placed at 35°C for continuous stirring for 24 h, and the obtained suspension was washed with deionized water for multiple centrifugal water (3500 r·min^{-1}, 5 min each time) until the pH of the supernatant was close to neutral. Then, the precipitate was dispersed in deionized water for 1.5 h, and then centrifuged at 3500 r·min^{-1} for 1 h to collect the dark green upper solution, which is the MXene dispersion. The upper solution is freeze-dried to obtain MXene powder.Take the top 0.1% of pixels from the dark channel map according to the brightness.

2.3 MoS_2-$Ti_3C_2T_x$ Preparation

Dissolve 78 mg tetrahydrate acid (AMT), 20 g $Ti_3C_2T_x$ MXene in 20 mL of ultrapure water and sonicate for 20 minutes. After that, 1 g of sulfur will be added and dissolved in the above solution. Transfer the solution to a hydrothermal reactor and react at 180 °C for 24 h. The reactor is cooled to room temperature, the product is washed three times by centrifugation, the black pellet of the lower layer is collected and freeze-dried. For comparison, keeping other conditions equal, MoS_2 was prepared without adding $Ti_3C_2T_x$MXene. By adjusting the AMT/$Ti_3C_2T_x$ ratio, different proportions of MoS_2-$Ti_3C_2T_x$ complexes were also obtained.

2.4 MoS_2-$Ti_3C_2T_x$/S Preparation

The MoS_2-$Ti_3C_2T_x$/S composite material uses melt diffusion method to mix MoS_2-$Ti_3C_2T_x$ composite and sulfur at a 1:2 mass ratio. The mixture is then added to a 155 °C drying oven and held for 12 h, then elevated to 300 °C and held for 2 h. After cooling to room temperature, MoS_2-$Ti_3C_2T_x$/S composites are obtained. In order to compare only $Ti_3C_2T_x$ powder, $Ti_3C_2T_x$/S composites were prepared by the same method.

2.5 Li_2S_6 Adsorption Experiment

Li_2S and sublimated sulfur were dissolved in a mixed solution of DOL/DEM (volume ratio 1:1) according to a molar ratio of 1:5, and then stirred for 12 h at 60 °C to obtain Li_2S_6 solution. $Ti_3C_2T_x$ and MoS_2-$Ti_3C_2T_x$ were added to a small glass bottle containing 3 mL of Li_2S_6 solution and allowed to stand for 12 h, and the adsorption of polysulfides was judged by observing the color change of the solution.

3. Results and Discussion

3.1 Morphological Phase Analysis of Materials

Ti_3AlC_2 was used as a precursor and it was treated in a mixed solution of LiF/HCI to etch the Al atomic layer. The etched multilayer $Ti_3C_2T_x$ was then ultrasonically peeled off, and then freeze-dried to obtain a few-layer sheet $Ti_3C_2T_x$ powder. As can be seen in Figure 1a, the initial Ti_3AlC_2 morphology is a lumpy structure, and the Ti_3AlC_2 obtained by etching is shown in Figure 1b, showing expansion and significantly increasing layer spacing. The morphology of MoS_2-$Ti_3C_2T_x$ is shown in Figure 3, and it can be clearly seen through the image that the layered stacking structure of $Ti_3C_2T_X$ is not obscured because MoS_2 is not covered by MoS_2 doping. The extremely small two-dimensional structure can make the rapid diffusion of lithium ions, and shorten the transfer channel distance of electrons in the positive electrode, so as to realize the rapid transfer of positive electrons.3.

Make a separate XRD for $Ti_3C_2T_x$ and compare it with the xrd of MoS_2-$Ti_3C_2T_x$. Compared with the (002) characteristic diffraction peak of $Ti_3C_2T_x$ at 6.8°, it was found that the (002) characteristic diffraction peak of MoS_2-$Ti_3C_2T_x$ was shifted, and it was shown at about 6.3° of the (002) diffraction surface of MXene, which means that $Ti_3C_2T_x$ expanded the layer spacing of the nanosheets after adding MoS_2 treatment, and the structure was well preserved.

ISSN: 2414-1895 DOI: 10.6919/ICJE.202304_9(4).0051

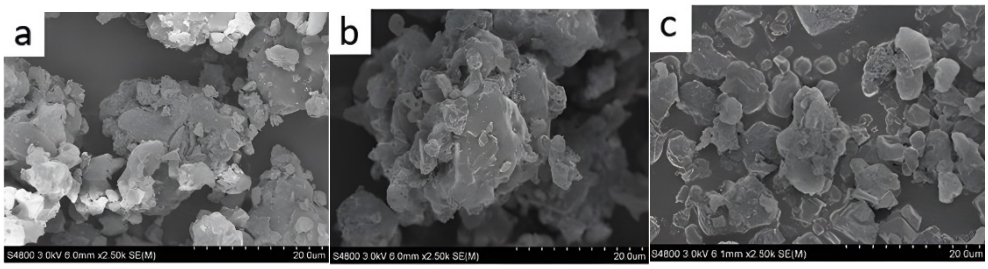

Fig 1. SEM images of (a) Ti_3AlC_2, (b) $Ti_3C_2T_x$, and (c) MoS_2-$Ti_3C_2T_x$

In order to further analyze the structural gap between Ti_3C_2Tx and MoS_2-$Ti_3C_2T_x$, we obtained XRD curves of $Ti_3C_2T_x$ and MoS_2-$Ti_3C_2T_x$ with the help of X-ray diffractometer, as shown in Figure 2. MXene's main crystal phase peak (002) is evident in both XRD curves, indicating that the structure of $Ti_3C_2T_x$ has not been damaged, consistent with SEM observations. Compared with the (002) characteristic diffraction peak of $Ti_3C_2T_x$ at 7.3°, the (002) characteristic diffraction peak of MoS_2-Ti_3C_2Tx doped with boron is shifted and displayed at about 7° of the (002) diffraction surface of MXene, which means that $Ti_3C_2T_x$ expands the layer spacing of the nanosheets after adding MoS_2 treatment, and the structure is well preserved.

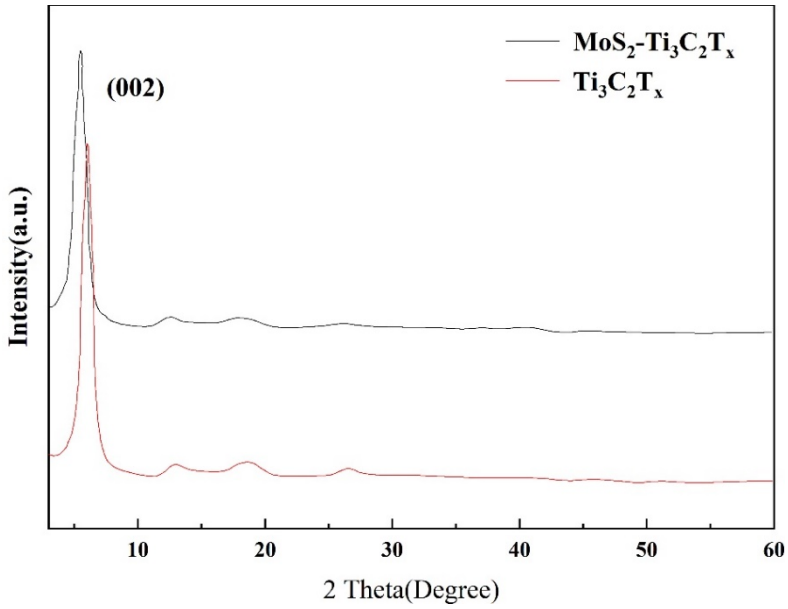

Fig 2. XRD patterns of $Ti_3C_2T_x$ and MoS_2-$Ti_3C_2T_x$

3.2 Structural Property Analysis of Materials

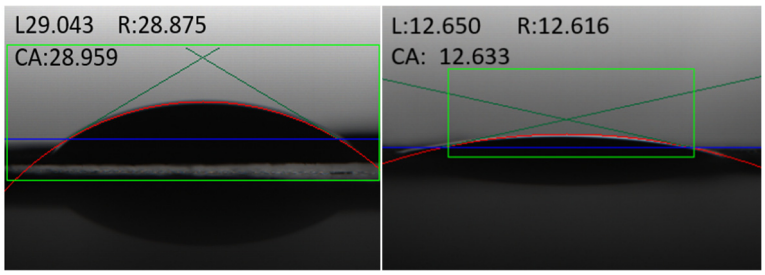

Fig 3. Contact angle test diagram of (a) $Ti_3C_2T_x$ and (b) MoS_2-$Ti_3C_2T_x$

In order to study the contact performance of the material and the electrolyte, $Ti_3C_2T_x$ and MoS_2-$Ti_3C_2T_x$ were tested on the contact angle of the electrolyte, and according to the test results of Figure 3, it was found that the angles obtained by Ti_3C_2Tx and MoS_2-$Ti_3C_2T_x$ were 29° (Figure 3a) and 12.6° (Figure 3b), respectively. The above data show that the affinity between MoS_2-Ti_3C_2Tx and the

ISSN: 2414-1895 DOI: 10.6919/ICJE.202304_9(4).0051

electrolyte is the best. Therefore, when MoS_2-$Ti_3C_2T_X$ is used as a positive electrode material, the electrolyte in the battery can be greatly retained and the internal resistance of the battery can be reduced, and it is conducive to reducing the internal resistance of the electrode and improving the electrochemical performance.

The addition of MoS_2 increases the specific surface area of $Ti_3C_2T_x$ and forms a unique structural advantage, which indicates that it can effectively improve the adsorption capacity of polysulfides. In order to visually verify this result, we have the adsorption effect of $Ti_3C_2T_x$ and MoS_2-$Ti_3C_2T_x$ on polysulfide (Li_2S_6). As shown in Figure 4, it can be clearly observed that after standing for 12 h, the color of both $Ti_3C_2T_x$(B) and MoS_2-$Ti_3C_2T_x$(A) solutions becomes lighter, but in contrast, the solution of MoS_2-$Ti_3C_2T_x$ is close to colorless, which proves that the addition of MoS_2 further improves the ability of $Ti_3C_2T_x$ to adsorb polysulfides.

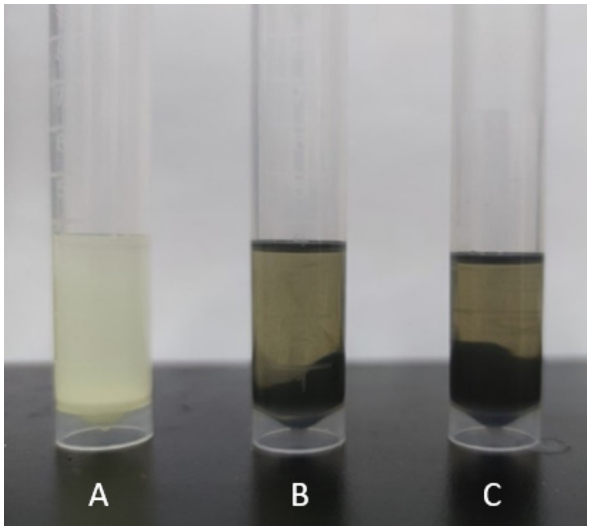

Fig 4. Li_2S_6 solution adsorption of $Ti_3C_2T_x$ and MoS_2-$Ti_3C_2T_x$

Through thermogravimetric analysis (TGA) testing, the sulfur content of $Ti_3C_2T_x$/S and MoS_2-$Ti_3C_2T_x$/S was tested to be 64.3 wt% and 71.6 wt%, respectively, as shown in Figure 5. It is also demonstrated that the addition of MoS_2 makes it have a larger specific surface area and pore volume, and to a certain extent, it is proved that the presence of MoS_2 enhances the adsorption of sulfur.

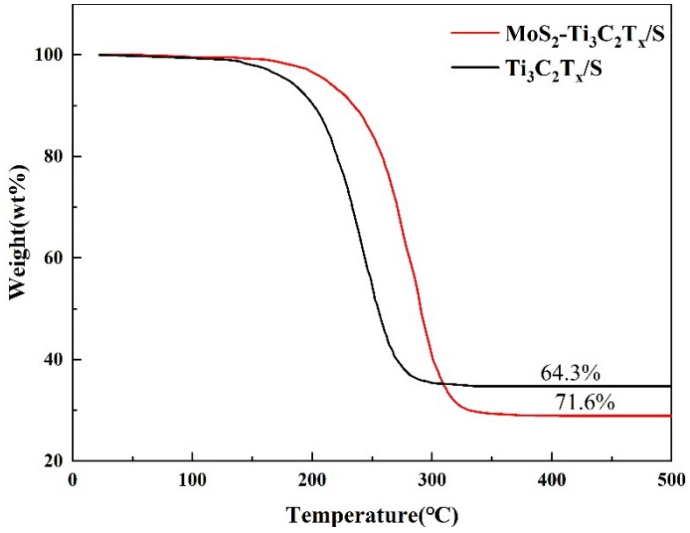

Fig 5. TGA curves of $Ti_3C_2T_x$/S and MoS_2-$Ti_3C_2T_x$/S

3.3 Electrochemical Test Analysis

The MoS_2-$Ti_3C_2T_x$/S, acetylene black and PVDF were evenly mixed in NMP according to the mass ratio of 8:1:1 to make a cathode slurry, and the resulting slurry was evenly coated on a better level,

ISSN: 2414-1895 DOI: 10.6919/ICJE.202304_9(4).0051

and dried in a vacuum drying oven at 60 °C for 12 h, and then cut into round pieces (diameter = 12 mm), weighed the quality of the positive electrode sheet, and put it in the glove box for later.

Assemble the battery in an argon atmosphere glove box with less than 1 ppm of water and oxygen content. The CR2025 model shell was selected, using a 16×0.4 mm metal lithium sheet as the negative electrode, the diaphragm used Celgard 2400 PP diaphragm, the electrolyte was a mixture of DME and DOL configured according to the ratio of 1:1 volume, 1 M LiTFSI was used as a lithium salt, and 0.1 M $LiNO_3$ was added. The positive electrode piece is placed in the middle of the positive electrode shell and the electrolyte is added dropwise, and the electrolyte is added dropwise after the positive electrode piece is completely wetted, and the metal lithium sheet, gasket, shrapnel, and battery shell are placed on the separator in turn, and the battery is sealed with a sealing machine, and the assembled battery needs to stand for 12 h, and test their electrochemical performance.

In order to study the effect of MoS_2-$Ti_3C_2T_x$ composite matrix materials on the electrochemical properties of sulfur, Figure 6 shows the cyclic voltammetry test of sulfur in $Ti_3C_2T_x$/S and MoS_2-$Ti_3C_2T_x$/S electrodes. It was performed at a scanning speed of 0.1 $mV \cdot s^{-1}$, as shown in Figure 6 as a cyclic voltammetry characteristic curve. From the experimental results, it can be seen that the composite electrode material of MoS_2-$Ti_3C_2T_x$/S has two reduction peaks, the first reduction peak is S to Li_2S_8, and the second reduction peak is Li_2S_8 to Li_2S_2 and Li_2S. At the scanning speed of 0.2 $mV \cdot s^{-1}$, two oxidation peaks appeared in the MoS_2-$Ti_3C_2T_x$/S electrode material with different proportions of sulfur content. This is the process of oxidation of Li_2S to S and electron transfer in the MoS_2-$Ti_3C_2T_x$ matrix material. From Figure 7, it can be seen that when the scanning speed increases, it is clear that only one oxidation peak remains. This is mainly due to the poor electrochemical activity of MoS_2-$Ti_3C_2T_x$ matrix material, and its electrochemical reaction rate decreases significantly with the increase of scanning speed.

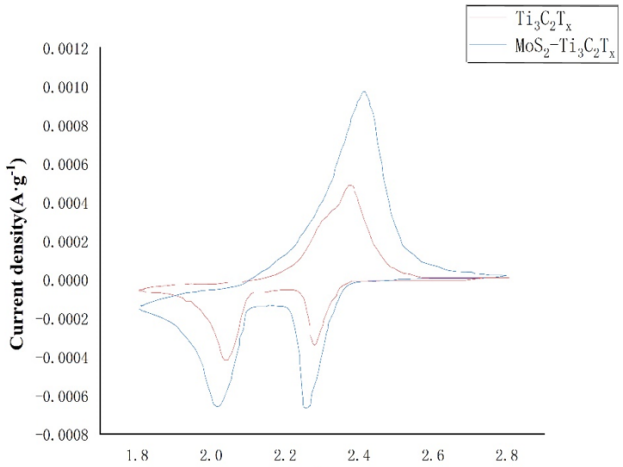

Fig 6. CV curves of $Ti_3C_2T_x$/S and MoS_2-$Ti_3C_2T_x$/S electrodes

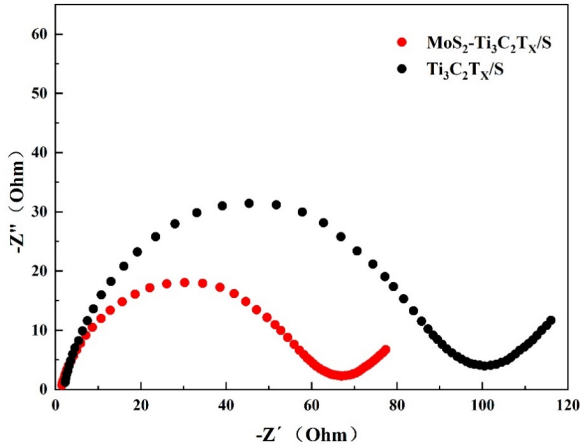

Fig 7. EIS spectra of $Ti_3C_2T_x$/S and MoS_2-$Ti_3C_2T_x$/S electrodes

ISSN: 2414-1895 DOI: 10.6919/ICJE.202304_9(4).0051

In order to compare the charge-discharge performance and cycling performance of $Ti_3C_2T_x$/S and MoS_2-$Ti_3C_2T_x$/S electrodes, we first tested the constant current charge-discharge at 0.2 C rate current. The results are shown in Figure 8, from which it can be seen that the curve has two discharge plates at approximately 2.3 and 2.1 V, which is related to the reduction of sulfur to long-chain polysulfides and further conversion to solid Li_2S_2/Li_2S, consistent with the CV curve results described above. At a charging platform of 2.3-2.4 V, lithium polysulfide is converted to sulfur. In addition, it can be seen from the figure that the discharge specific capacity of the MoS_2-$Ti_3C_2T_x$/S electrode is higher than that of the $Ti_3C_2T_x$/S electrode (1055.5 $mAh \cdot g^{-1}$ and 898.4 $mAh \cdot g^{-1}$, respectively), and the polarization of the MoS_2-$Ti_3C_2T_x$/S electrode is smaller than that of the $Ti_3C_2T_x$/S electrode. The higher specific capacity and lower polarization of the MoS_2-$Ti_3C_2T_x$/S electrode are due to the effective anchoring of boron doping and the improved sulfur utilization rate of polysulfide reuse, as well as the higher cell reaction kinetics, which is consistent with the result of higher redox peaks in the CV curve. In addition, as shown in Figure 9, the MoS_2-$Ti_3C_2T_x$/S electrode showed better cycle stability in the cyclic charge-discharge test, and the discharge specific capacity of the MoS_2-$Ti_3C_2T_x$/S electrode was 755 $mAh \cdot g^{-1}$ after 100 cycles, which was 71.6% of the initial specific capacity, which was better than the discharge specific capacity and 65.9% retention rate of 592 $mAh \cdot g^{-1}$ of $Ti_3C_2T_x$/S electrode.

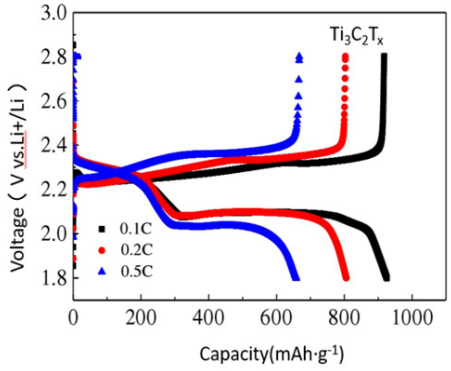

Fig 8. Charge-discharge curve of $Ti_3C_2T_x$/S electrode

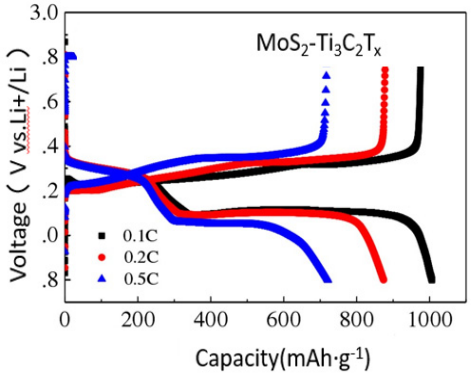

Fig 9. Charge-discharge curve of MoS_2-$Ti_3C_2T_x$/S electrode

4. Conclusion

In this paper, MoS_2-$Ti_3C_2T_x$/S doped with MXene was successfully prepared by MoS_2 and hydrothermal method as a cathode composite. MoS_2-$Ti_3C_2T_x$ material retains the advantages of large specific surface area and pore volume of $Ti_3C_2T_x$ material, and does not block the active site, which not only effectively improves the diffusion of lithium ions, but also shortens the transfer distance of electrons and promotes the reaction kinetics. The structural properties of the materials showed that the doping of MoS_2 enhanced the adsorption inhibition of polysulfides, and the sulfur content in the composites was as high as 70.2%. The MoS_2-$Ti_3C_2T_x$/S electrode achieves excellent electrochemical

ISSN: 2414-1895 DOI: 10.6919/ICJE.202304_9(4).0051

performance: the initial discharge specific capacity of 1057 $mAh \cdot g^{-1}$ is obtained at 0.2 C, and it remains at 758.3 $mAh \cdot g^{-1}$ after 100 cycles, which is 71.7% of the initial discharge capacity, and the discharge specific capacity of the MoS_2-$Ti_3C_2T_x$/S electrode has excellent rate performance and cycle stability. The strategies and experimental results proposed in this paper provide a reference scheme for improving the energy density of lithium-sulfur batteries.

References

[1] Pourvakhshoori Negar,Poursadeghiyan Mohsen,Khankeh Hamid Reza,Harouni Gholamreza Ghaedamini,Farrokhi Mehrdad. The simultaneous effects of thermal stress and air pollution on body temperature of Tehran traffic officers.[J]. Journal of environmental health science & engineering, 2020, 18(1). Y.X. Li, H.S.Yu: Research on Image Dehazing by Fusion of Dark Channel and MSRCR Algorithm (Modern Computer), Vol. 2022, No. 28, p. 24-33.

[2] Bhavani Palagiri,Hussain Murid,Park Young-Kwon. Recent advancements on the sustainable biochar based semiconducting materials for photocatalytic applications: A state of the art review[J]. Journal of Cleaner Production,2022,330. D.Y. Shi, J.L. Zhang and B. Jia: Nie Ling, Yang Huimin.Research on Vehicle License Plate Image Dehazing Method Based on Improved Dark Channel Prior (Applications of Electronic Technology), Vol. 2022 No. 48, p.13-18.

[3] Xiaolei Wang. Hierarchical Carbon Nanosheet Arrays for Lithium Metal Batteries and Electrochemical Water Splitting[J]. ECS Meeting Abstracts,2020,MA2020-01(5). W. Li, J.B. Yang and T. Sun: Fu Lingling.Retinex based multi-scale single image defogging network (Journal of Qingdao University), Vol. 2022 No. 35, p.26-32.

[4] Jesse Hinricher,Michael Julian Orella,Jeffrey A Kowalski,Fikile R. Brushett. Quantifying Decay Rates of Electrochemically Active Species Using Microelectrode Voltammetry[J]. ECS Meeting Abstracts, 2020, MA2020-01(3). Y.H. Zhang, Z.H. Li and Z.H. Xie: Qin R J.Improvement of real-time image defogging algorithm based on FPGA (Changjiang Information Communication), Vol. 2022 No. 35, p.66-68.

[5] Natsuho Kazahaya,Yu Katayama,Hiromori Tsutsumi. Contribution of Metal Additives on the Electrochemical Process Involving Solid Sulfur and Soluble Lithium Polysulfide in Lithium-Sulfur Batteries[J]. ChemElectroChem,2021,8(11). Z.H. Si, P. Yu and Y. Wang: Single Image Fusion Dehazing Algorithm Based on Dark Channel (Computer Applications and Software), Vol. 2022 No. 39, p.240-284.

[6] Zhang Zhi-yuan,Liu Zheng,Sarah Burangi. A Floating Garbage Disposal Vessel[J]. Journal of Applied Science and Engineering Innovation,2019,6(1). B.W. Li, J.F. Liu: Review of image defogging technology (Modern Computer), Vol. 2022 No. 28, p.57-61.

[7] Kweon Hyukmin,KimShoemaker William. Mitigating Lithium Dissolution and Polysulfide Shuttle Effect Phenomena Using a Polymer Composite Layer Coating on the Anode in Lithium–Sulfur Batteries[J]. Polymers,2022,14(20).

[8] Naguib M, Kurtoglu M,Presser V, et al. Two-dimensional nanocrystals produced byexfoliat ion of Ti3AlC2 [J]. Advanced Materials, 2011, 23 (37): 4248-4253.

[9] Zhao Q, Zhu Q, Liu Y, et al. Status and Prospects of MXene-Based Lithium-Sulfur Batteries[J]. Advanced Functional Materials, 2021, 31(21): 1-28.

[10] Wang X, Yang C, Xiong X, et al. A robust sulfur host with dual lithium polysulfide immobilization mechanism for long cycle life and high capacity Li-S batteries[J]. Energy Storage Materials, 2019, 16: 344-353.

[11] Igor V. Koptyug. Applications of NMR tomography to mass transfer studies[J]. Russian Chemical Reviews, 2002,71(10).